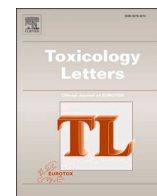| Title	Generation and application of CES1-knockout Tet-Off-regulated CYP3A4 and UGT1A1-expressing Caco-2 cells
Author(s)	Murata, Michika; Okada, Kentaro; Takahashi, Masaki et al.
Citation	Toxicology Letters. 2024, 401, p. 158-169
Version Type	VoR
URL	https://hdl.handle.net/11094/98590
rights	This article is licensed under a Creative Commons Attribution-NonCommercial-NoDerivatives 4.0 International License.
Note	

Generation and application of CES1-knockout Tet-Off-regulated CYP3A4 and UGT1A1-expressing Caco-2 cells

Michika Murata [a], Kentaro Okada [b,d], Masaki Takahashi [c], Yukiko Ueyama-Toba [a,d,e], Sumito Ito [c], Hiroyuki Mizuguchi [a,b,d,e,f,g,*]

[a] Laboratory of Biochemistry and Molecular Biology, Graduate School of Pharmaceutical Sciences, Osaka University, Osaka 565-0871, Japan
[b] Laboratory of Biochemistry and Molecular Biology, School of Pharmaceutical Sciences, Osaka University, Osaka 565-0871, Japan
[c] GenoMembrane Co., Ltd., 2-3-18 Namamugi, Tsurumi-ku, Yokohama, Kanagawa 230-0052, Japan
[d] Laboratory of Functional Organoid for Drug Discovery, National Institutes of Biomedical Innovation, Health and Nutrition, Osaka 567-0085, Japan
[e] Integrated Frontier Research for Medical Science Division, Institute for Open and Transdisciplinary Research Initiatives, Osaka University, Osaka, Japan
[f] Global Center for Medical Engineering and Informatics, Osaka University, Osaka 565-0871, Japan
[g] Center for Infectious Disease Education and Research (CiDER), Osaka University, Osaka 565-0871, Japan

ARTICLE INFO

ABSTRACT

Caco-2 cells, a human colorectal adenocarcinoma cell line, are widely used to model small intestinal epithelial cells in the drug development process because they can predict drug absorption with high accuracy. However, Caco-2 cells have several issues. First, Caco-2 cells have little expression of cytochrome P450 3A4 (CYP3A4), which is a major drug-metabolizing enzyme in the human intestine. We previously developed Caco-2 cells whose expression of CYP3A4 can be controlled using doxycycline (Dox) (CYP3A4-Caco-2 cells) (Ichikawa et al., Sci. Rep, 2021). However, since the Tet-On system was used to regulate CYP3A4 expression in these cells, there was concern about drug-drug interactions. The second issue is that in the human small intestine, carboxylesterase 2 (CES2) is more highly expressed than carboxylesterase 1 (CES1), while in Caco-2 cells CES1 is more highly expressed. The third issue is the low level expression of uridine diphosphate glucuronosyltransferase 1A1 (UGT1A1), a phase II drug-metabolizing enzyme. In this study, we used genome-editing technology to establish *CES1*-knockout Caco-2 cells whose CYP3A4 and UGT1A1 expression can be regulated by the Tet-Off system. These cell lines would be useful in pharmaceutical researches, including intestinal toxicological studies, as an in vitro model for orally administered drugs.

1. Introduction

Orally administered drugs are first absorbed and metabolized in the small intestine before being transported to the liver, where they undergo further metabolism, and then enter systemic circulation. Because the small intestine expresses various drug transporters and drug-metabolizing enzymes, these proteins have a significant impact on the bioavailability of orally administered drugs. The absorption of drugs in the small intestine is determined not only by passive diffusion but also by active transporters such as peptide transporter 1 (*PEPT1*) and efflux transporters such as multi-drug resistance 1 (*MDR1*) that mediate active transport and excretion, respectively (Giacomini et al., 2010). Moreover, drugs taken up by intestinal epithelial cells are metabolized by drug-metabolizing enzymes such as cytochrome P450 3A4 (*CYP3A4*)

(Paine et al., 2006). Therefore, the evaluation of absorption, metabolism, and excretion in the small intestine is important for predicting the bioavailability of orally administered drugs (Doherty and Charman, 2002; Nauli and Nauli, 2013).

Because obtaining and culturing primary human small intestinal epithelial cells is very difficult, in vitro absorption model systems such as parallel artificial membrane permeability assay (PAMPA), Madin-Darby canine kidney cells (MDCK cells), and human colorectal adenocarcinoma cells (Caco-2 cells) have been widely used. However, PAMPA cannot evaluate the influence of drug-metabolizing enzymes and drug transporters since it is an artificial lipid membrane model (Nishimuta et al., 2011). MDCK cells which overexpress pharmacokinetics-related genes such as *CYP3A4* and *MDR1* have been reported (Jin et al., 2014; Kataoka et al., 2013; Kwatra et al., 2012; Mease et al., 2012), but they

---

Fig. 1. Establishment of CES1-KO Caco-2 cells. (**A**) A schematic overview of the targeting strategy for CES1 is shown. (**B**) PCR was performed to confirm the insertion of a universal NHEJ self-cleaving targeting plasmid in the *CES1* locus. (**C**) PCR was performed to confirm the deletion of the sequence between two gRNAs in the *CES1* locus. (**D**) The gene expression levels of *CES1* in WT Caco-2 cells and CES1-KO Caco-2 cells were measured by qRT-PCR. The gene expression levels of *GAPDH* were taken as 1.0. All data are represented as means ± SD (*n*=3). Statistical significance was evaluated by unpaired two-tail Student's t test (***p < 0.005). (**E**) The CES1 protein expression levels in WT Caco-2 cells and CES1-KO Caco-2 cells were measured by western blotting analysis. (**F**) Immunofluorescence staining of CES1 (red) was performed in WT Caco-2 cells and CES1-KO Caco-2 cells. Nuclei were counterstained with DAPI (blue). Scale bars represent 50 μm.

are derived from kidney cells of dogs and may not accurately predict the drug pharmacokinetics in humans. Caco-2 cells, which are derived from human colorectal adenocarcinoma, form a structure similar to that of columnar epithelial cells with microvilli and form tight junctions when cultured on a cell culture insert (Sun et al., 2008; Yamashita et al., 2002). They express various drug transporters, and the membrane permeability coefficient (*Papp*) of orally administered drugs in Caco-2 cells correlates with the fraction absorbed (*Fa*) in the human intestine (Artursson et al., 2001; Takenaka et al., 2016). Therefore, Caco-2 cells are widely used as a model that can predict the *Fa* value of orally administered drugs.

However, there are at least three issues associated with the use of
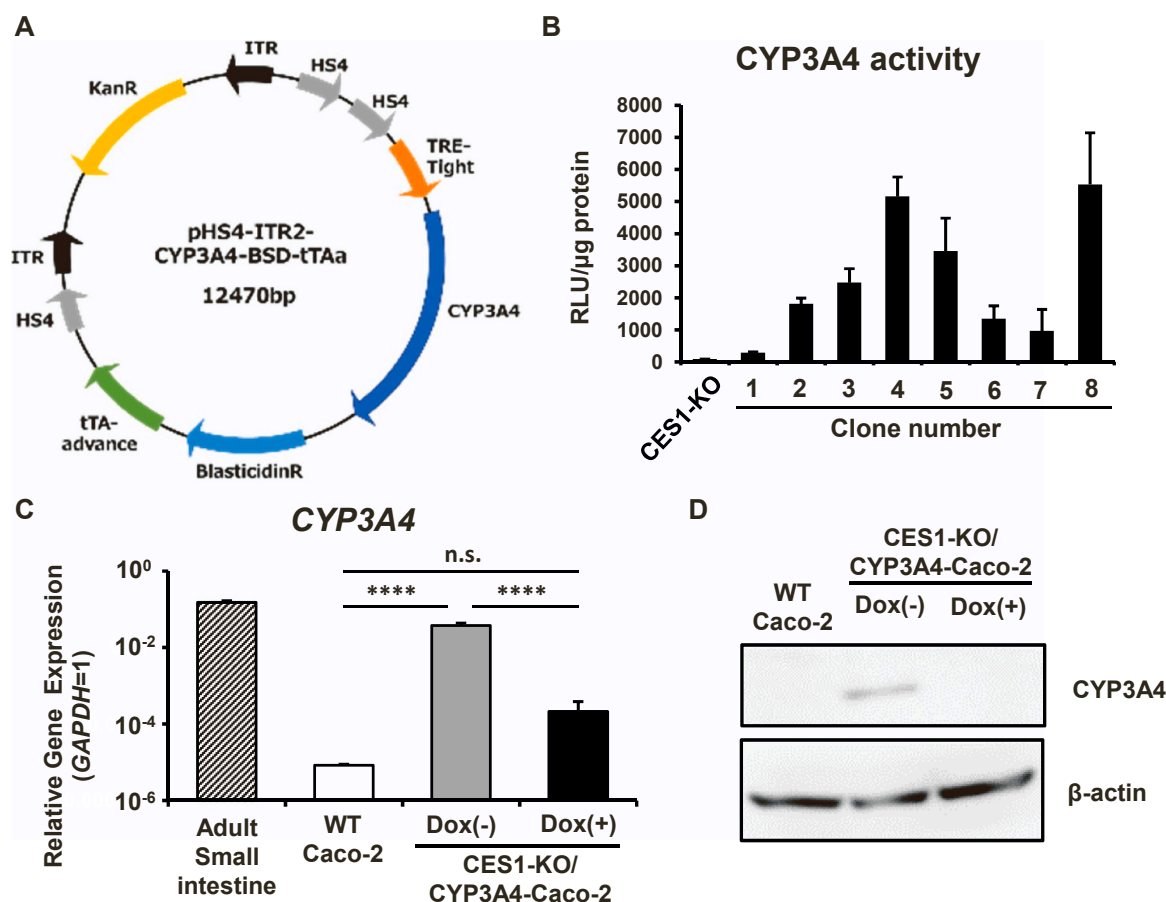
Fig. 2. Establishment of CES1-KO/CYP3A4-Caco-2 cells. (**A**) A vector map of pHS4-ITR2-CYP3A4-BSD-tTAa. (**B**) The CYP3A4 activity levels were measured in nine clones of CES1-KO/CYP3A4-Caco-2 cells. (**C**) The gene expression levels of *CYP3A4* in the adult small intestine, WT Caco-2 cells and CES1-KO/CYP3A4-Caco-2 cells with or without Dox were measured by qRT-PCR. The gene expression levels of *GAPDH* were taken as 1.0. Statistical significances were evaluated by one-way ANOVA followed by Tukey's post-hoc tests (****$p < 0.001$). All data are represented as means ±S.D. (n=3). (**D**) The CYP3A4 protein expression levels in WT Caco-2 cells and CES1-KO/CYP3A4-Caco-2 cells with or without Dox were measured by western blotting analysis.

Caco-2 cells as model for human intestinal metabolism and transport. The first is the significantly low expression and activity of CYP3A4 (Prueksaritanont et al., 1996). CYP3A4 is the most prominent species of the CYP3A family, whose members are involved in the metabolism of over half of all drugs that undergo oxidation(Wilkinson, 2005). Additionally, the CYP3A family accounts for approximately 80 % of CYPs expressed in the small intestine(Paine et al., 2006). Therefore, predicting the intestinal first-pass metabolism (*Fg*) using Caco-2 cells is difficult. Although several groups have attempted to establish Caco-2 cells that stably express CYP3A4, the activity levels of CYP3A4 were still lower than in intestinal cells, and has not yet been realized for accurately predicting metabolism by CYP3A4 in the small intestine has not been realized(Brimer-Cline and Schuetz, 2002; Crespi et al., 1996; Hu et al., 1999; Negoro et al., 2022; Takenaka et al., 2017). We previously succeeded in establishing Caco-2 cells that express CYP3A4 using the *PiggyBac* transposon system (Ichikawa et al., 2021). Their CYP3A4 metabolizing activity was comparable to that in human intestinal tissue in vivo (Ichikawa et al., 2021). However, since the Tet-On system was used for the control of CYP3A4 expression, there were concerns regarding drug-drug interactions between doxycycline (Dox) and the test compound. The second is that the expression profile of carboxylesterase (CES) is different between human small intestine and Caco-2 cells. In human small intestine, carboxylesterase 2 (*CES2*) is more highly expressed than carboxylesterase 1 (*CES1*) (Taketani et al., 2007), yet in Caco-2 cells, *CES1* is more highly expressed than *CES2* (Imai et al., 2005b). In other words, the expression ratio of CES1 and CES2 in the human small intestine is the inverse of that in Caco-2 cells. CES is a

drug-metabolizing enzyme that metabolizes ester-based drugs, with CES1 and CES2 being representative enzymes, and many prodrugs are known to be metabolized by CES (IMAI, 2006). CES1 metabolizes drugs with bulky acyl groups, such as oseltamivir, while CES2 metabolizes drugs with bulky alcohol groups, such as irinotecan (Ishizaki et al., 2018). Therefore, to improve prediction of bioavailability of orally administered ester-containing drugs, it is necessary to control the expression ratio of CES1 and CES2 in Caco-2 cells. The third issue is the low expression level of uridine diphosphate glucuronosyltransferase 1A1 (*UGT1A1*), a phase II drug-metabolizing enzyme. UGT1A1 is highly expressed in the small intestine and is suggested to be significantly involved in the bioavailability of several orally administered drugs (Fisher et al., 2001). It has also been reported that UGT1A1 is involved in the enterohepatic circulation of drugs such as irinotecan (de Man et al., 2018), and the gastrointestinal toxicity of irinotecan and its metabolites, SN-38 and SN-38G, is known as an important side effect. Thus to improve prediction of intestinal uptake of UGT1A1 substrates, it would be beneficial to develop an intestinal model system representing UGT1A1 activity.

In this study, we attempted to establish Caco-2 cells with Tet-off system-mediated controllable expression of CYP3A4 using a transposon-based gene transfer system, in addition to knocking out the CES1 gene using the CRISPR-Cas9 system. Then, we evaluated whether the established cells can be used for drug metabolism tests. Finally, we established and evaluated CES1-KO-Caco-2 cells that co-express CYP3A4 and UGT1A1.

2. Material and methods

2.1. Culture of Caco-2 cells

Caco-2 cells (ATCC, HTB-37) were cultured in Minimum Essential Medium Eagle (MEM, Sigma, Missouri) supplemented with 10 % fetal bovine serum (FBS), 1 % Non-Essential Amino Acid Solution (NEAA) (Thermo Fisher Scientific, Massachusetts), Penicillin-Streptomycin (Nacalai Tesque, Japan), and 2 mM L-glutamine (Nacalai Tesque). For differentiation, Caco-2 cells were seeded onto BD Falcon Cell Culture Inserts (24-well, 0.4-μm pore size, 353095; Corning, New York) at a density of 2.5×10^5 cells/cm^2 and cultured for 21 days.

2.2. Plasmids

The plasmid expressing Streptococcus pyogenes Cas9 (SpCas9) and guide RNA (gRNA) was generated by ligating double-stranded oligonucleotides into the *Bbs*I site of pX330 (Addgene no. 42230; provided by Dr. Feng Zhang at Massachusetts Institute of Technology)(Cong et al., 2013). Another plasmid expressing SpCas9 and gRNA was generated by ligating double-stranded oligonucleotides into the *Bbs*I site of pX459 (Addgene, no 48139, provided by Dr. Feng Zhang at Massachusetts Institute of Technology)(Ran et al., 2013). For knockout of *CES1* gene, gRNA sequences shown in Supplemental Table 1 were inserted into pX330, resulting in pX330-CES1-gRNA1&2. A universal NHEJ self-cleaving targeting plasmid was previously generated (Shintani et al., 2023). For linearization of universal non-homologous end joining (NHEJ) self-cleaving targeting plasmids, gRNA sequences shown in Supplemental Table 1 were inserted into pX459, resulting in pX459-NHEJ-gRNA1&2&3. The schematic diagram for CES1-KO was shown in Fig. 1A.

A transposase expression plasmid, pHMEF-PB, was constructed by insertion of the sequence of Transposase(Yusa et al., 2011), which was synthesized by artificial gene synthesis (Twist Bioscience, California), into pHMEF5(Kawabata et al., 2005). A CYP3A4 expression plasmid, pHS4-ITR2-CYP3A4-BSD-tTAa (Fig. 2A), was constructed by the conventional cloning technique using restriction enzymes and ligation. The coding sequences of CYP3A4 and HS4 (Chung et al., 1993) (chicken β-globin insulator) were determined by referencing from GeneBank NM_017460 and U78775.2, respectively. The coding sequences of tTA advance and the TRE-tight promoter were determined by referencing from manufacture's information (Clontech, California). These sequences were synthesized by artificial gene synthesis (Azenta Life Sciences, New Jersey). Further details on the construction method are available upon request.

2.3. Generation of CES1-KO Caco-2 cells

To knock out *CES1* gene expression by genome editing technology, Caco-2 cells were first treated with 10 μM valproic acid for 24 h (Takayama et al., 2017), then detached with trypsin and electroporated with pX330-CES1-gRNA1&2, pX459-NHEJ-gRNA1&2&3 and the universal NHEJ self-cleaving targeting plasmid using NEPA21 (Nepa Gene, Japan). After electroporation, the cells were cultured in MEM and replaced 2 days later with MEM containing 10 μM puromycin (Thermo Fisher Scientific). After 14 days of electroporation, colonies were picked and seeded in individual wells of a 12-well plate. Genotyping was performed by PCR after each well reached confluent.

2.4. Generation of Caco-2 Cells containing Tet-Off-regulated CYP3A4 expression cassette

Caco-2 cells (3.0×10^5 cells/well in a 6-well plate) were transfected with pHS4-ITR2-CYP3A4-BSD-tTAa and pHMEF-PB using Lipofectamine 2000 (Thermo Fisher Scientific). The following day, the cells were detached, seeded in a 100 mm dish, and selection was performed by adding 4 μg/mL of blasticidin S hydrochloride (FUJIFILM Wako, Japan). Colonies were picked and the cells were propagated.

2.5. Quantitative RT-PCR

RNA extraction from cells was performed using Sepasol RNA I Super G (Nacalai Tesque) and cDNA synthesis was performed using the Superscript VILO cDNA synthesis kit (Thermo Fisher Scientific). Quantitative RT-PCR (qRT-PCR) was performed using SYBR Green PCR Master Mix (Thermo Fisher Scientific) on a StepOnePlus real-time PCR system (Thermo Fisher Scientific). The expression levels of the target genes were normalized to the expression levels of the housekeeping gene (glyceraldehyde 3-phosphate dehydrogenase (*GAPDH*)). The primer sequences used are shown in Supplemental Table 3. Total RNA - Human Adult Normal Tissue 5 Donor Pool: Small Intestine (BioChain Institute, Inc. California) was used as a positive control for small intestine.

2.6. Western blotting

Western blotting was performed according to our previous report (Ichikawa et al., 2021). All antibodies used in this paper are described in Supplementary Table 4.

2.7. Fluorescent immunostaining

Caco-2 cells cultured on Cell Culture Inserts for 21 days were fixed by treating them with 4 % paraformaldehyde at room temperature for 15 min, followed by washing with PBS. Blocking was performed with PBS containing 2 % BSA and 0.2 % TritonX-100 (Sigma-Aldrich) for 15 min. After incubation with primary antibodies at 4°C overnight, the cells were washed with PBS and then incubated with secondary antibodies and DAPI at room temperature for 1 h. The cells were observed using BIOREVO BZ-9000 (KEYENCE, Japan). The antibodies used are shown in Supplemental Table 5.

2.8. Luminescent CYP3A4 activity assay

CYP3A4 activity was measured using P450-GloTM CYP3A4 Assay Kits (Promega, Wisconsin). Luciferin-IPA was used as the substrate for CYP3A4, and luminescence was measured using a luminometer (Lumat LB 9507, Berthold). CYP3A4 activity was corrected for the protein amount in each well.

2.9. Native-PAGE Coupled with Esterase Staining

CES activity staining was performed according to previous reports (Imai et al., 2005a). Briefly, cells were washed with PBS and suspended in SET buffer (240 mM sucrose, 1 mM EDTA-2Na, 10 mM Tris-HCl (pH=7.4)). The cell suspension was sonicated, and the total protein content of Caco-2 cells was extracted. The supernatant was collected by centrifugation at 9000 g, 4°C for 30 min, and the S9 fraction was prepared and stored at −80°C. The protein content in each S9 fraction was quantified using Protein Assay Dye Reagent Concentrate (BioRad, California). A S9 fraction containing 30 μg of protein was mixed with solubilization buffer (135 mM Tris-HCl (pH=6.8), 0.002 % p-nitrophenol, 20 % glycerol, 0.75 % Nonidet-P40) in equal amounts, applied to a 7.5 % polyacrylamide gel, and subjected to Native-PAGE at 100 V using an electrophoresis buffer (1 % Nonidet P-40, 192 mM glycine, 25 mM Tris). The activity of CES was evaluated by staining the gel with CES activity staining solution (2.659 mM α-naphthyl acetate in 1 % acetonitrile, 0.962 mM Fast Red TR salt, 100 mM Na-K phosphate buffer (pH=7.0)) using α-naphthyl acetate as the substrate.

2.10. Calculation of the apparent membrane permeability (Papp)

The apparent membrane permeability (Papp) was calculated using

the following equation:

$$Papp = \delta Cr / \delta t \times Vr / (A \times C0)$$

δCr = final receiver concentration; δt = assay time; Vr = receiver volume

A = Cell culture insert growth area; C_0 = concentration in the donor compartment.

2.11. Permeability and CES1 metabolism assay using Enalapril

Caco-2 cells cultured on Cell Culture inserts for 21 days were treated with 0.25 mL of Hank's Balanced Salt Solution (HBSS; Thermo Fisher Scientific) on the apical side and 1 mL on the basolateral side. The cells were then pre-incubated at 37°C for 30 min. After the pre-incubation, 10 µM enalapril was added to the apical side, and 2 h later the solution were collected from the apical and basolateral sides. The cells were also collected at the same time, and the collected cell solution was frozen and thawed to disrupted cells. The concentrations of enalapril and enalaprilat in each fraction were measured using LC-MS/MS.

2.12. CYP3A4 metabolism assay using Midazolam and testosterone

Caco-2 cells cultured on Cell Culture inserts for 21 days were washed with PBS and then treated with a solution containing 5 µM final concentration of Midazolam (FUJIFILM Wako) and 100 µM final concentration of Testosterone (FUJIFILM Wako) in HBSS. Two hour later, the supernatant was collected and protein was denatured with acetonitrile (FUJIFILM Wako). The concentrations of 1′-hydroxymidazolam (1′-OH MDZ) and 6β-hydroxy testosterone (6β-OH TES) in the culture supernatant were measured using liquid chromatography-tandem mass spectrometry (UPLC-MS/MS; Waters). The amounts of 1′-hydroxymidazolam and 6β-hydroxy testosterone formed were calculated from the measured values and corrected for the total protein amount per well.

2.13. Measurement of Trans-Epithelial Electrical Resistance (TEER)

TEER values were measured by Millicell-ERS2 (Merck Millipore). Caco-2 cells and their derivatives were cultured on Cell Culture Inserts from day 0 of differentiation. The raw data were converted to $\Omega \times cm^2$ based on the culture insert area (0.4 cm^2).

2.14. Lucifer yellow permeation test

Differentiated Caco-2 cells cultured on Cell Culture inserts were washed with HBSS. Then, 0.25 mL of HBSS with or without 10 mM capric acid (C10; Sigma-Aldrich) and 1.0 mL of HBSS solution was added to the apical and basolateral side, respectively, of the Cell Culture insert, and the cells were incubated for 30 min at 37 °C. After the incubation, 100 µM Lucifer Yellow (LY; FUJIFILM Wako) was added to the apical side and allowed to act for 90 min, and the amount of LY that permeated from the apical side to the basolateral side was quantified. The obtained sample was diluted twice with HBSS, and the fluorescence intensity was measured using a TriStar LB941 (Berthold Technologies, Germany) with an excitation wavelength (Ex) of 485 nm and an emission wavelength (Em) of 535 nm.

2.15. Evaluation of transport activity of MDR1 and BCRP

The transport activity of MDR1 and BCRP was evaluated using Digoxin[3 H] (PerkinElmer, Massachusetts) and Estrone sulfate[14 C], respectively. First, HBSS solution was added to the apical side and basolateral side of Caco-2 cells cultured on Cell Culture inserts for 21 days, and incubated for 30 min at 37°C. Then, HBSS containing 1 µM Digoxin or 10 µM Estron sulfate[14 C]was added to either the apical or basolateral side (donor side), and HBSS without a substrate compound was added to the opposite compartment (receiver side). After incubation for 90 min at 37°C, the sample was collected from the receiver side.

Verapamil and Ko143 were used as inhibitors of MDR1 and BCRP, respectively, and added to the apical side, respectively. The concentration of Digoxin[3 H] and Estrone sulfate[14 C] in the samples was quantified using a microplate scintillation/luminescence counter MicroBeta2 (PerkinElmer).

The efflux ratio (ER) was calculated using the following equation:

$$ER = Papp \ (B \ to \ A) / Papp \ (A \ to \ B)$$

Papp (A to B): Papp from the apical side to the basolateral side

Papp (B to A): Papp from the basolateral side to the apical side

2.16. UGT1A1 metabolism test using SN-38

Caco-2 cells cultured on Cell Culture inserts for 21 days were washed with PBS and then treated with a solution containing 1 µM final concentration of SN-38 (FUJIFILM Wako) in HBSS. Two hours later, the supernatant was collected and protein was denatured with acetonitrile (FUJIFILM Wako). The concentrations of SN-38 glucuronide (SN-38G) in the culture supernatant were measured using liquid chromatography-tandem mass spectrometry (UPLC-MS/MS; Waters). The production amounts of SN38G was calculated from the measured values and corrected for the total protein amount per well.

3. Results

3.1. Establishment of CES1-KO Caco-2 cells

To establish Caco-2 cells with CES1 gene knockout, we targeted Exon5 of the *CES1* gene, which contains the active site Ser residue for *CES1*, and performed genome editing using the CRISPR-Cas9 system. We used a method in which a donor plasmid, which had been cut by CRISPR-Cas9 to form a linear structure, was inserted into the site where the *CES1* gene was cut by the double-stranded break and repaired by non-homologous end joining (NHEJ)(Artegiani et al., 2020) (Fig. 1A). Positive selection with puromycin was performed, and 18 Caco-2 cell clones were obtained. Genotyping was then performed to confirm the insertion of the sequence derived from donor plasmid at the *CES1* gene locus in the obtained Caco-2 cell clones. The primers used for genotyping were designed to amplify a band of 0.9 kbp for the wild-type allele and a band of 5.4 kbp for the allele with the donor plasmid inserted (Table S2, Fig. 1A,B). A clone with the donor plasmid inserted was obtained.

To analyze the allele that did not show donor insertion, primers were designed near the gRNA site and amplified by PCR. It was confirmed that the sequence in the clone with the donor plasmid inserted was about 133 bp shorter than that in the WT Caco-2 cells, which corresponds to the length between the two gRNAs, suggesting a deletion between the two gRNAs (Fig. 1A,C). The cells of this clone were named CES1-KO Caco-2 cells and further analyzed.

To confirm the *CES1* knockout, mRNA and protein expression analyses were performed. qRT-PCR analysis showed a significant decrease in *CES1* gene expression in CES1-KO Caco-2 cells (Fig. 1D). Western blotting analysis showed a disappearance of the CES1-specific band in CES1-KO Caco-2 cells (Fig. 1E). Similar results were obtained in immunofluorescence staining (Fig. 1F). These results indicate the successful establishment of CES1-KO Caco-2 cells.

3.2. Establishment of CES1-KO/CYP3A4-Caco-2 cells

To establish CYP3A4-expressing Caco-2 cells in which CES1 had been knocked out, we used transposase on the CES1-KO Caco-2 cells established as shown in Fig. 1. We co-transfected CES1-KO Caco-2 cells with pHS4-ITR2-CYP3A4-BSD-tTAa (Fig. 2A) and pHMEF-PB, a transposase
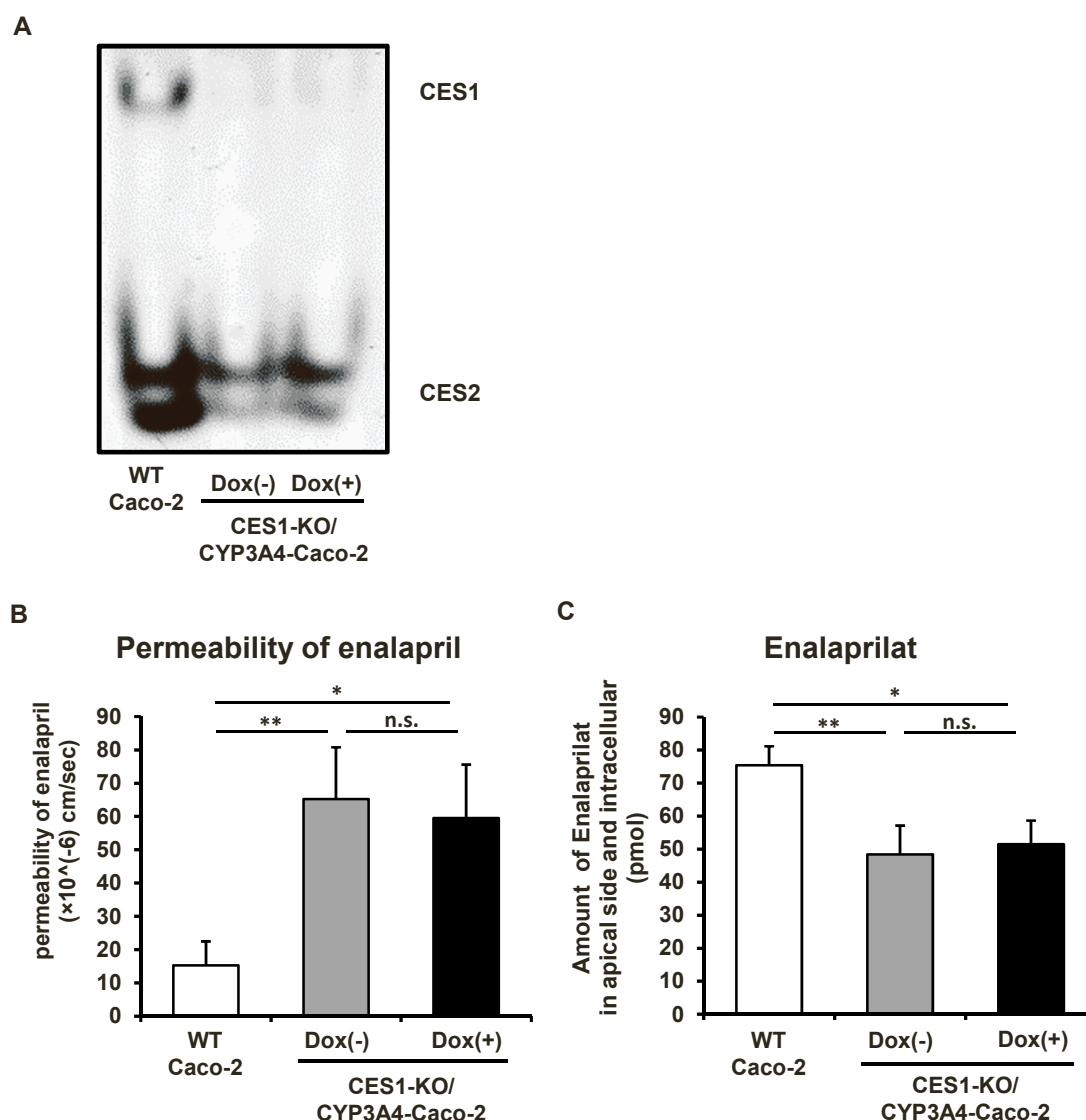
Fig. 3. Evaluation of the drug metabolizing activity of CES in CES1-KO/CYP3A4-Caco-2 cells. (**A**) Polyacrylamide gel electrophoresis of the S9 fraction (30 µg of protein) of WT Caco-2 cells and CES1-KO/CYP3A4-Caco-2 cells with or without Dox, followed by staining for esterase activity using α-naphtyl acetate. (**B**) The apical-to-basal permeability of enalapril across the WT Caco-2 monolayers and CES1-KO/CYP3A4-Caco-2 monolayers with or without Dox was measured. Statistical significances were evaluated by one-way ANOVA followed by Tukey's post-hoc tests ($*p < 0.05$, $**p < 0.01$). Data are presented as means ± SD (n=3). (**C**) The amounts of enalaprilat on the apical side and within the cells of the WT Caco-2 monolayers and CES1-KO/CYP3A4-Caco-2 monolayers with or without Dox were measured. Statistical significances were evaluated by one-way ANOVA followed by Tukey's post-hoc tests ($*p < 0.05$, $**p < 0.01$). Data are presented as means ± SD (n=3).

expression plasmid, and performed positive selection using blasticidin S. After selection, nine Caco-2 cell clones were obtained. To confirm the expression of CYP3A4 in the nine Caco-2 cell clones, we measured CYP3A4 activity in the absence of doxycycline (Dox). The results showed that the expression of CYP3A4 could be regulated by the Tet-Off system. Significant CYP3A4 activity was observed in clones 4, 5, and 8 compared to cells without gene transfer (Fig. 2B). Subsequently, the cells of clone 8 were named CES1-KO/CYP3A4-Caco-2 cells, and analysis was performed.

To determine whether CES1-KO/CYP3A4-Caco-2 cells expressed CYP3A4, we analyzed the mRNA and protein expressions. In addition, we examined whether CYP3A4 expression was regulated by the Tet-Off system. A significant increase in *CYP3A4* gene expression was confirmed in CES1-KO/CYP3A4-Caco-2 cells without Dox (Fig. 2C). Western blotting showed that a specific band of CYP3A4 was observed only in CES1-KO/CYP3A4-Caco-2 cells without Dox (Fig. 2D). Thus, we successfully established CES1-KO Caco-2 cells expressing CYP3A4 (CES1-KO/CYP3A4-Caco-2 cells).

3.3. Evaluation of CES activity in CES1-KO/CYP3A4-Caco-2 cells

Additional analyses were performed to evaluate CES1 activity in established CES1-KO/CYP3A4-Caco-2 cells. First, CES activity staining was performed using native-PAGE to evaluate the metabolic capacities of CES1 and CES2. Bands corresponding to CES1 and CES2 activities were detected in WT Caco-2 cells, indicating the presence of both activities. In contrast, in CES1-KO/CYP3A4-Caco-2 cells with or without Dox, the CES1 band disappeared and only the CES2 band was detectable (Fig. 3A). These results suggested that CES1 expression was lost in CES1-KO/CYP3A4-Caco-2 cells, while CES2 activity was maintained. Next, enalapril, a CES1 substrate, was used to evaluate CES1 activity. Enalapril is a prodrug that is modified by ester bonds to enalaprilat and is a substrate for the apical absorption transporter PEPT1 (Temple and Boyd, 1998). In the human small intestine, enalapril is absorbed via PEPT1 without undergoing metabolism by CES1. However, in Caco-2 cells, enalapril undergoes CES1-mediated metabolism to enalaprilat and is subsequently excreted from the cells to both the apical and basolateral
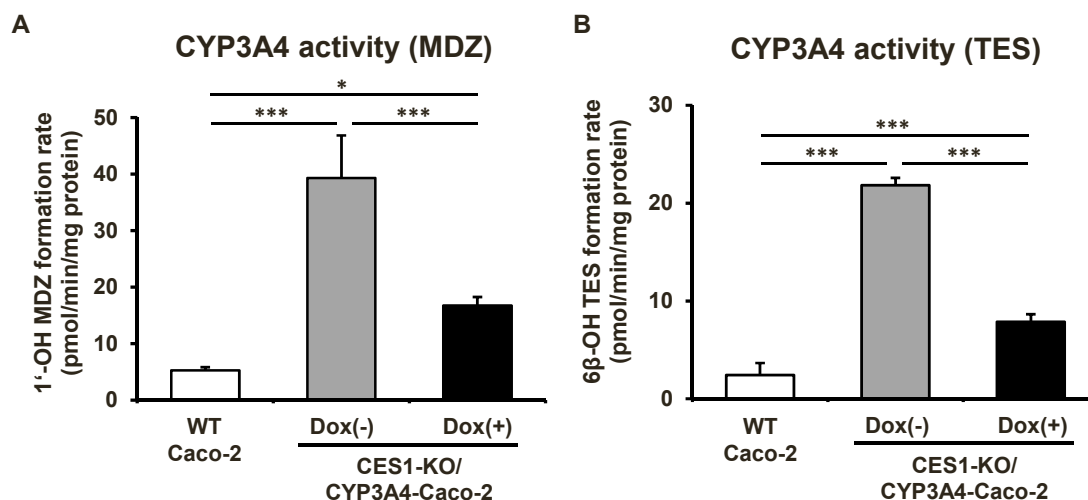
A

CYP3A4 activity (MDZ)

B

CYP3A4 activity (TES)

Fig. 4. Evaluation of the drug metabolizing activity of CYP3A4 in CES1-KO/CYP3A4-Caco-2 cells. The CYP3A4-mediated drug-metabolizing capacities in WT Caco-2 cells and CES1-KO/CYP3A4-Caco-2 cells with or without Dox were evaluated by quantifying the metabolites of midazolam **(A)** and testosterone **(B)**. The quantities of 1'-hydroxymidazolam (A) and 6β-hydroxy testosterone (B) were measured by UPLC-MS/MS, respectively. Statistical significances were evaluated by one-way ANOVA followed by Tukey's post-hoc tests ($*p < 0.05$, $***p < 0.005$). All data are represented as means ± SD (n=4).

sides. Since enalaprilat is no longer a substrate for PEPT1 when excreted on the apical side, it was expected that the membrane permeability coefficient of Caco-2 cells would decrease (Thomsen et al., 2014). Indeed, the result showed that the membrane permeability coefficient of enalapril in CES1-KO/CYP3A4-Caco-2 cells was significantly increased compared to that in the WT Caco-2 cells (Fig. 3B). To investigate the cause of the increased absorption, the amount of enalaprilat, the expected CES1-metabolite, was measured. The amounts of enalaprilat present on the apical side and inside the cells were significantly lower in CES1-KO/CYP3A4-Caco-2 cells compared to WT Caco-2 cells (Fig. 3C). These findings suggest that CES1-KO/CYP3A4-Caco-2 cells could be used to improve evaluation of intestinal absorption of CES1-sensitive prodrugs.

3.4. Evaluation of CYP3A4 activity in CES1-KO/CYP3A4-Caco-2 cells

Further analysis was performed to evaluate the metabolic capacity of CYP3A4 in CES1-KO/CYP3A4-Caco-2 cells. The CYP3A4 activity was measured using the CYP3A4 substrates, midazolam and testosterone. The production of 1'-hydroxymidazolam, a metabolite of midazolam, was significantly increased in CES1-KO/CYP3A4-Caco-2 cells without Dox, compared to that in the WT Caco-2 cells. In addition, in CES1-KO/CYP3A4-Caco-2 cells with Dox, the production of 1'-hydroxymidazolam was significantly decreased compared to that without Dox (Fig. 4A). In the case of the metabolic measurement using testosterone, the production of 6β-hydroxy testosterone, a metabolite, was significantly increased in CES1-KO/CYP3A4-Caco-2 cells without Dox, compared to that in the WT Caco-2 cells (Fig. 4B). These results suggest that CES1-KO/CYP3A4-Caco-2 cells maintain CYP3A4 activity under the control of the Tet-off system. Thus, CES1-KO/CYP3A4-Caco-2 cells have the potential to predict the metabolism of orally administered drugs involving CYP3A4 in the small intestine.

3.5. Off-target analysis of pharmacokinetics-related gene expressions in CES1-KO/CYP3A4-Caco-2 cells

Gene expression analysis by qRT-PCR was performed to investigate off-target effects on the expression of pharmacokinetics-related genes in CES1-KO/CYP3A4-Caco-2 cells. First, gene expression analysis of drug metabolizing enzymes was performed using qRT-PCR in WT-Caco-2 cells and CES1-KO/CYP3A4-Caco-2 cells with or without Dox. The expression levels of the *CYP2C9* and *CES2* genes were not significantly different

between WT Caco-2 cells and CES1-KO/CYP3A4-Caco-2 cells. Expression of the *UGT1A1* gene was increased 12-fold in CES1-KO/CYP3A4-Caco-2 cells compared to WT Caco-2 cells (Fig. S1A). Next, gene expression analysis of drug transporters was performed. The expression levels of *OATP2B1* and *PEPT1* genes were not significantly different between WT Caco-2 cells and CES1-KO/CYP3A4-Caco-2 cells. The expression levels of *MDR1* and *MRP3* genes were increased 65-fold and 5-fold in CES1-KO/CYP3A4-Caco-2 cells compared to WT Caco-2 cells respectively. Expression of the *BCRP*, *MRP2* and *OATP1A2* genes was significantly decreased by approximately 50 %, 70 % and 40 %, respectively, in CES1-KO/CYP3A4-Caco-2 cells compared to WT Caco-2 cells (Fig. S1B). Finally, gene expression analysis of nuclear receptors involved in the induction of pharmacokinetics-related genes was performed. No significant difference in expression of the *FXR* and *PXR* genes was detected between WT Caco-2 cells and CES1-KO/CYP3A4-Caco-2 cells. The expression level of the *CDX2* gene was significantly decreased in CES1-KO/CYP3A4-Caco-2 cells compared to WT Caco-2 cells (Fig. S1C). Based on these results, it was suggested that the genome editing and forced insertion of the CYP3A4 expression cassette into the chromosome had off-target effect on the expression levels of pharmacokinetics-related genes.

3.6. Off-target analysis of monolayer membrane function in CES1-KO/ CYP3A4-Caco-2 cells

Various analyses were conducted to investigate off-target effects on monolayer membrane function in CES1-KO/CYP3A4-Caco-2 cells resulting from genomic modifications. First, trans-epithelial electrical resistance (TEER) was measured to confirm the ability of monolayer formation. The results showed that both the WT Caco-2 cells and CES1-KO/CYP3A4-Caco-2 cells with or without Dox exhibited values of 800–950 $\Omega \cdot cm^2$, suggesting that monolayer formation ability was not impaired by the genomic modifications (Fig. 5A). The membrane permeability coefficient (Papp) was determined using Lucifer yellow, a compound known to only pass through the intercellular space. The results showed that Papp was 1.30–1.90×10^{-6} cm/s, and that the addition of capric acid (C10), an absorption enhancer, increased Papp (Fig. 5B). This Papp value met the FDA recommended criterion for a monolayer membrane for drug permeation testing (0.2–2×10^{-6} cm/s) ("Drug Interaction Studies Design, Data Analysis, and Implication for Dosing and Labeling").

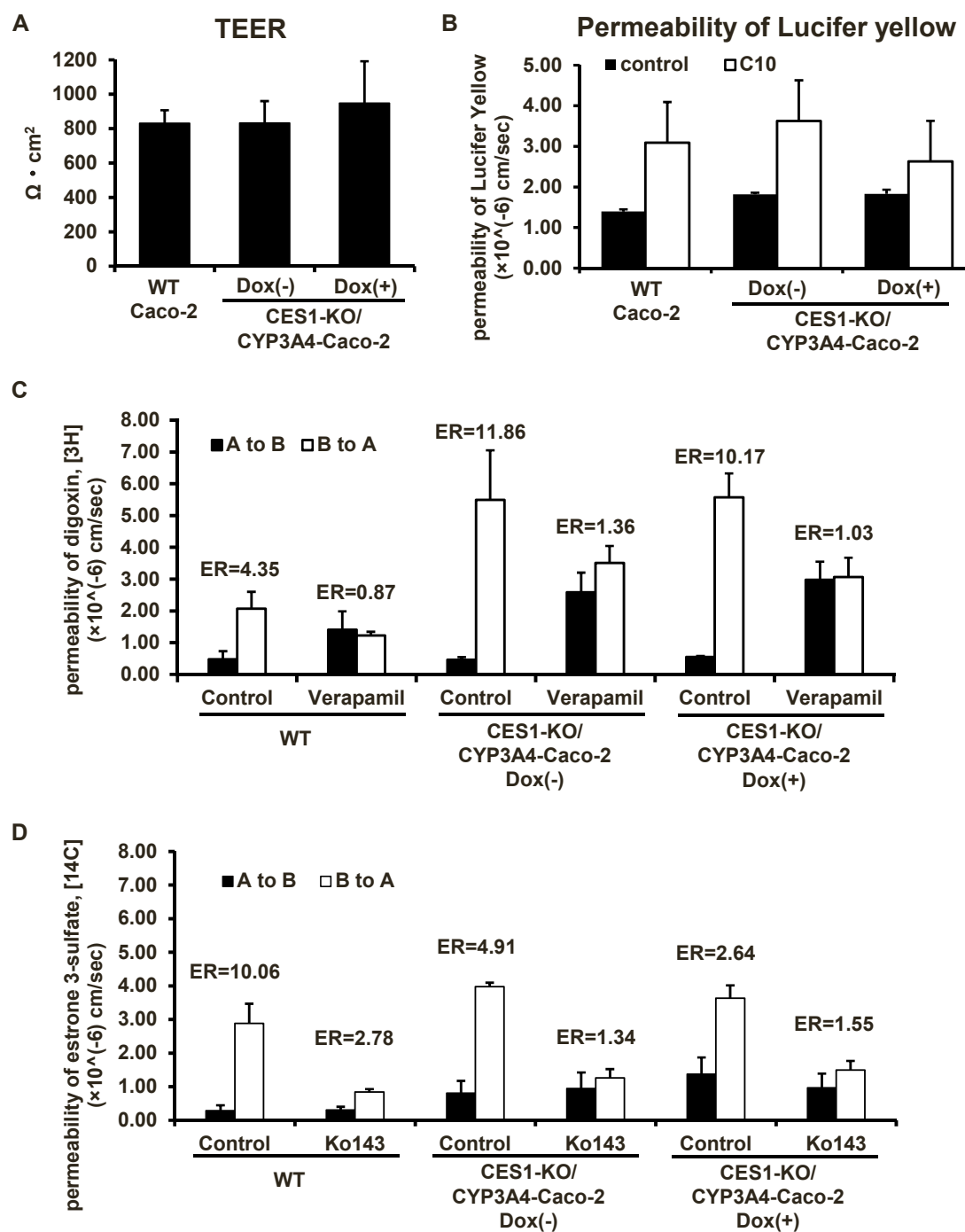Next, the transporter activity of MDR1 was evaluated using digoxin,

Fig. 5. Off-target analysis of CES1-KO/CYP3A4-Caco-2 cells to monolayer functions. **(A)** The TEER values of WT Caco-2 cells and CES1-KO/CYP3A4-Caco-2 cells with or without Dox were measured by Millicell-ERS2 to evaluate monolayer formation ability. **(B)** The *Papp* values of Lucifer yellow in the WT Caco-2 cells and CES1-KO/CYP3A4-Caco-2 cells with or without Dox were measured. The *Papp* value was also measured for the group to which C10, an absorption enhancer, was added. **(C)** Evaluation of P-gp activity using digoxin [3 H]. Permeation from the apical side to the basolateral side (A to B) is shown in the black columns, while that from the basolateral side to the apical side (B to A) is shown in the white columns. The efflux ratio (ER) of each group is shown above the columns. **(D)** Evaluation of BCRP activity using estrone 3-sulfate [14 C]. Permeation from the apical side to the basolateral side (A to B) is shown in the black columns, and that from the basolateral side to the apical side (B to A) is shown in the white columns. The efflux ratio (ER) of each group is shown above the columns. Data are presented as means ± SD (n=3).

a known substrate for MDR1. The results showed that both the WT Caco-2 cells and CES1-KO/CYP3A4-Caco-2 cells with or without Dox exhibited an efflux ratio (ER value) of 4 or more, confirming the activity of MDR1. This result was in line with the increased mRNA expression reported in the previous session (Fig. S1B). The inhibition of MDR1 by verapamil, a known MDR1 inhibitor, was also confirmed (Fig. 5C). The transporter activity of BCRP was also evaluated using estron 3-sulfate, a

known substrate for BCRP. The results showed that both the WT Caco-2 cells and CES1-KO/CYP3A4-Caco-2 cells with or without Dox exhibited an efflux ratio (ER value) of 2 or more, confirming the transporter activity of BCRP. The inhibition of BCRP by Ko143, a known BCRP inhibitor, was confirmed (Fig. 5D). The decreased ER from 10.06 (WT control) to 4.91 and 2.64 (CES1-KO/CYP3A4-Caco-2 cells without or with Dox, respectively) appeared to be due to the 3–4 increase of A to B
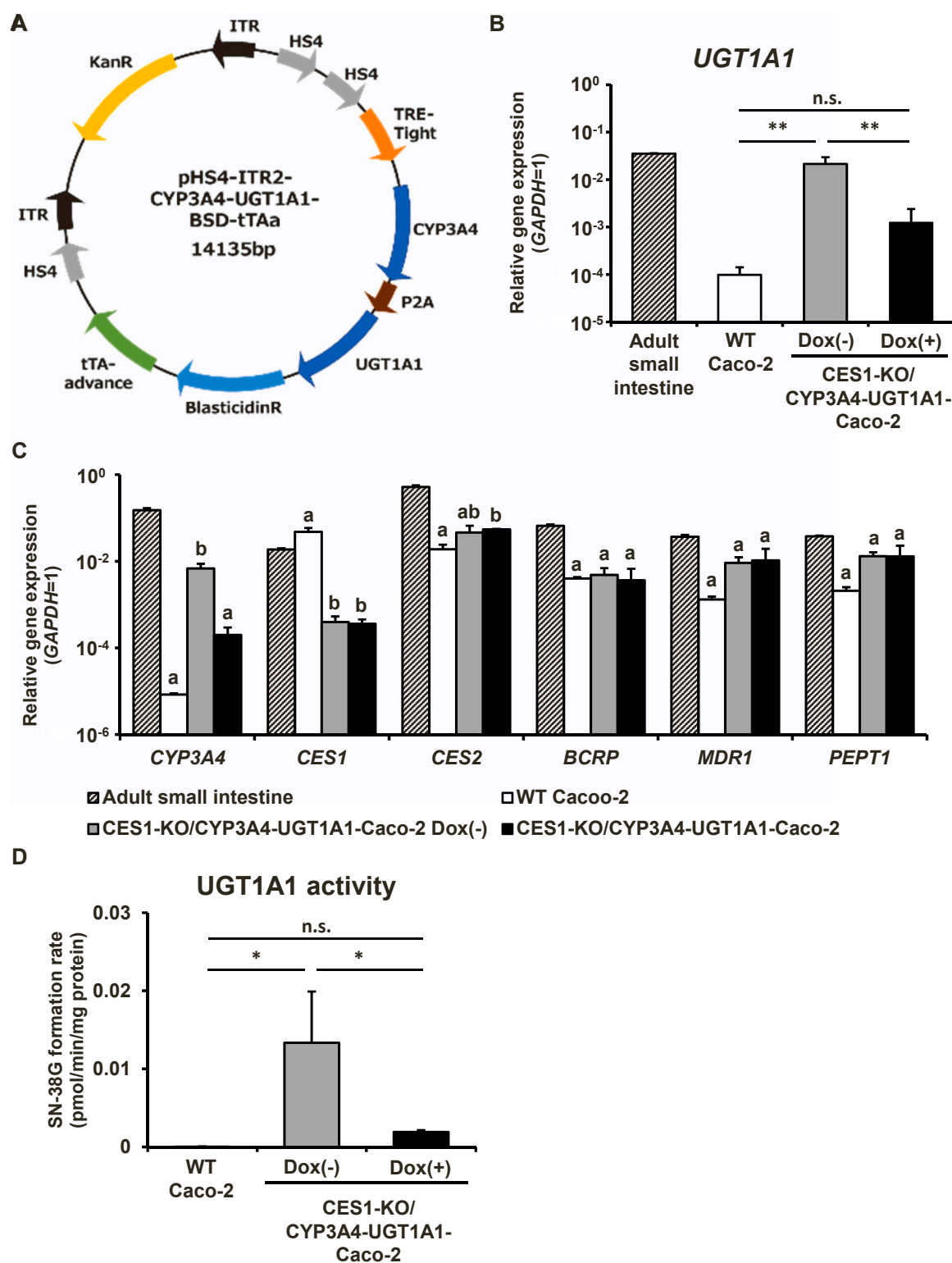
Fig. 6. Generation and functional analysis of CES1-KO/CYP3A4-UGT1A1-Caco-2 cells. **(A)** A vector map of pHS4-ITR2-CYP3A4-UGT1A1-BSD-tTAa. **(B)** The gene expression levels of *UGT1A1* in the adult small intestine, WT Caco-2 cells and CES1-KO/CYP3A4-UGT1A1-Caco-2 cells with or without Dox were measured by qRT-PCR. The gene expression levels of *GAPDH* were taken as 1.0. Statistical significances were evaluated by one-way ANOVA followed by Tukey's post-hoc tests (**$p < 0.01$). All data are represented as means ±S.D. (n=3). **(C)** The gene expression levels of *CYP3A4, CES1, CES2, BCRP, MDR1* and *PEPT1* in WT Caco-2 cells and CES1-KO/CYP3A4-UGT1A1-Caco-2 cells with or without Dox were measured by qRT-PCR. On the y axis, the gene expression levels of *GAPDH* were taken as 1.0. Statistical significances were evaluated by one-way ANOVA followed by Tukey's post-hoc tests ($p < 0.05$). Groups that do not share the same letter are significantly different from each other. All data are represented as means ±S.D. (n=3). **(D)** The UGT1A1-mediated drug-metabolizing capacities in WT Caco-2 cells and CES1-KO/CYP3A4-UGT1A1-Caco-2 cells with or without Dox were evaluated by quantifying the metabolites of SN-38. The quantity of SN-38G was measured by UPLC-MS/MS. Statistical significances were evaluated by one-way ANOVA followed by Tukey's post-hoc tests (*$p < 0.05$). All data are represented as means ± SD (n=3).

transport, which was consistent with the down-regulation of BCRP-expression mentioned in the previous session (Fig. S1B). Therefore, CES1-KO/CYP3A4-Caco-2 cells were suggested to maintain the transporter activity of both MDR1 and BCRP. In conclusion, neither genome editing nor overexpression of CYP3A4 affected monolayer membrane function in CES1-KO/CYP3A4-Caco-2 cells.

3.7. Establishment and functional analysis of CES1-KO/CYP3A4-UGT1A1-Caco-2 cells

We further tried to introduce *UGT1A1* genes into CES1-KO/CYP3A4-Caco-2 cells. We transfected CES1-KO Caco-2 cells with pHS4-ITR2-CYP3A4-UGT1A1-BSD-tTAa (Fig. 6A) and pHMEF-PB, a transposase expression plasmid, and carried out positive selection with blasticidin S. Seven Caco-2 cell clones were obtained following selection. We performed qRT-PCR analysis to confirm the introduction of *CYP3A4* and *UGT1A1* genes in the transfected cells. One of the clonal cell lines was subsequently designated CES1-KO/CYP3A4-UGT1A1-Caco-2 cells and subjected to further analysis. Gene expression analysis showed a significant increase in *UGT1A1* and *CYP3A4* gene expression in CES1-KO/CYP3A4-UGT1A1-Caco-2 cells compared to that in WT-Caco-2 cells. *CES1* gene expression was significantly decreased in CES1-KO/CYP3A4-UGT1A1-Caco-2 cells compared to WT-Caco-2 cells. There was no significant difference in the expression levels of the *CES2*, *BCRP*, *MDR1*, and *PEPT1* genes between the two cell types (Fig. 6B,C). To examine the metabolic activity of UGT1A1, we performed a metabolic assay using SN-38, a UGT1A1 substrate. The results showed a significant increase in the production of SN-38G, a metabolite of SN-38, in the CES1-KO/CYP3A4-UGT1A1-Caco-2 cells compared to the WT-Caco-2 cells in the non-Dox treated group. However, in the Dox-treated group, the production of SN-38G was equivalent to that in WT-Caco-2 cells (Fig. 6D).

4. Discussion

In this study, we successfully established Caco-2 cells in which CES1 was knocked out and CYP3A4 expression was controlled by the Tet-off system. Although there have been reports of Caco-2 cells expressing CYP3A4, the cell lines established in these studies were not practical because their CYP3A4 activity was insufficient and not lasting (Brimer-Cline and Schuetz, 2002; Crespi et al., 1996; Hu et al., 1999; Negoro et al., 2022; Takenaka et al., 2017). We previously established Caco-2 cells expressing CYP3A4 using the PiggyBac Transposon system (Ichikawa et al., 2021). However, these cells required the addition of Dox for CYP3A4 expression, raising concerns about drug interactions between Dox and drugs subjected to kinetic testing. The CES1-KO/CYP3A4-Caco-2 cells established in this study do not require the addition of Dox for CYP3A4 expression, overcoming the issue in our previous work. In addition, we knocked out the CES1 gene in Caco-2 cells. CES enzymes are responsible for the metabolism of ester-based drugs and are involved in the metabolism of prodrugs such as enalapril (McLeod et al., 1986). The absorption of these prodrugs in the small intestine might not be accurately predicted due to metabolism by CES1, which is highly expressed in Caco-2 cells. The CES1-KO/CYP3A4-Caco-2 cells showed the potential to overcome this problem (Fig. 3B, C). We further attempted to construct a new in vitro intestinal model by co-expressing the CYP3A4 and UGT1A1 genes in CES1-KO Caco-2 cells. Since UGT1A1 plays an important role in drug metabolism but is expressed at low levels in Caco-2 cells, we established CES1-KO CYP3A4/UGT1A1-Caco-2 cells.

While we were preparing for this manuscript, a similar study was reported (Yamada et al., 2023). However, since the CES1-KO/CYP3A4-Caco-2 and CES1-KO/CYP3A4-UGT1A1-Caco-2 cells in the present study can regulate the expression levels of CYP3A4 and UGT1A1 by Dox, our system would have an advantage over the system developed by Yamada et al. In particular, the ability to prepare control cells that express little CYP3A4 or UGT1A1 merely by adding Dox,

without the need to prepare separate control (wild-type) cells, represents an important advantage of our system.

The CES1-KO/CYP3A4-Caco-2 cells have the potential to predict the absorption of prodrugs modified for greater absorption in the small intestine (Fig. 3B,C), and to predict the metabolism of drugs involving CYP3A4 (Fig. 4). In addition, CES1-KO/CYP3A4-Caco-2 cells with UGT1A1 activity were successfully established (Fig. 6). In the future, it will be necessary to investigate whether the Caco-2 cells, established in this study, can accurately predict the value of Fa×Fg in the human small intestine, which represents absorption, metabolism, and excretion, by examining the correlation between Fa×Fg in the human small intestine and *Papp* of some drugs in the established Caco-2 cells.

We examined only 13 off-target genes related to pharmacokinetics in this study. As there are many drug-metabolizing enzymes and drug transporters, it is necessary to investigate more genes using techniques such as RNA-Seq. CES2 activity decreased in CES1-KO/CYP3A4-Caco-2 cells(Fig. 3A). On the other hands, CES2 mRNA expression level not changed in CES1-KO/CYP3A4-Caco-2 cells(Fig6C). It remained unclear about this phenomenon.

Finally, we should note two important issues in regard to the CES1-KO/CYP3A4-Caco-2 and CES1-KO/CYP3A4-UGT1A1-Caco-2 cells developed herein. First, the expression of several pharmacokinetic-related genes showed variability. This phenomenon may have arisen as a result of inherent characteristics unique to each individual clone. Variances in properties among clones are commonly observed(Horie et al., 2003). The second issue was that both CES1-KO/CYP3A4-Caco-2 and CES1-KO/CYP3A4-UGT1A1-Caco-2 cells had still low levels of CYP3A4 and UGT1A1 expression in the presence of Dox, which is common for a tetracycline-regulated system. Due to the distinct characteristics of each of these clones, acquiring a larger number of clones would enable the identification of superior clones with less leakiness and increased inducibility. Since transposons can forcibly transfer and integrate genes into the cellular genomes, it would be easy to obtain many stable overexpression cell lines for this purpose.

5. Conclusion

We established CES1-KO/CYP3A4-Caco-2 and CES1-KO/CYP3A4-UGT1A1-Caco-2 cells. These cell lines will contribute to the advancement of drug discovery research, including intestinal toxicological studies, as an in vitro evaluation system for orally administered pharmaceuticals.

Author Contributions

MM and HM designed the experiments; MM, KO, TM, and SI performed the experiments; MM and Y.U-T analyzed the data; MM and HM wrote the manuscript; HM approved the manuscript

CRediT authorship contribution statement

Hiroyuki Mizuguchi: Writing – review & editing, Supervision, Resources, Project administration, Investigation, Funding acquisition, Conceptualization. **Sumito Ito:** Data curation. **Yukiko Ueyama-Toba:** Formal analysis. **Masaki Takahashi:** Investigation. **Kentaro Okada:** Investigation, Data curation. **Michika Murata:** Writing – review & editing, Writing – original draft, Visualization, Validation, Methodology, Investigation, Formal analysis, Data curation, Conceptualization.

Declaration of Competing Interest

The authors declare no conflict of interest

Data Availability

Data will be made available on request.

Appendix A. Supporting information

Supplementary data associated with this article can be found in the online version at doi:10.1016/j.toxlet.2024.10.003.

References

Artegiani, B., Hendriks, D., Beumer, J., Kok, R., Zheng, X., Joore, I., Chuva de Sousa Lopes, S., van Zon, J., Tans, S., Clevers, H., 2020. Fast and efficient generation of knock-in human organoids using homology-independent CRISPR–Cas9 precision genome editing. Nat. Cell Biol. 22, 321–331. https://doi.org/10.1038/s41556-020-0472-5.

Artursson, P., Palm, K., Luthman, K., 2001. Caco-2 monolayers in experimental and theoretical predictions of drug transport. Adv. Drug Deliv. Rev. 46, 27–43. https://doi.org/10.1016/S0169-409X(00)00128-9.

Brimer-Cline, C., Schuetz, E.G., 2002. Polarized cell cultures for integrated studies of drug metabolism and transport. Methods Enzymol. 357, 321–329. https://doi.org/10.1016/S0076-6879(02)57690-4.

Chung, J.H., Whiteley, M., Felsenfeld, G., 1993. A 5′ element of the chicken β-globin domain serves as an insulator in human erythroid cells and protects against position effect in Drosophila. Cell 74, 505–514. https://doi.org/10.1016/0092-8674(93)80052-G.

Cong, L., Ran, F.A., Cox, D., Lin, S., Barretto, R., Habib, N., Hsu, P.D., Wu, X., Jiang, W., Marraffini, L.A., Zhang, F., 2013. Multiplex genome engineering using CRISPR/Cas systems. Science 339 (80), 819–823. https://doi.org/10.1126/science.1231143.

Crespi, C.L., Penman, B.W., Hu, M., 1996. Development of Caco-2 cells expressing high levels of cDNA-derived cytochrome P4503A4. Pharm. Res. 13, 1635–1641. https://doi.org/10.1023/A:1016428304366.

Doherty, M.M., Charman, W.N., 2002. The Mucosa of the small intestine. Clin. Pharmacokinet. 41, 235–253. https://doi.org/10.2165/00003088-200241040-00001.

Fisher, M.B., Paine, M.F., Strelevitz, T.J., Wrighton, S.A., 2001. The role of hepatic and extrahepatic UDP-glucuronosyltransferases in human drug metabolism*†. Drug Metab. Rev. 33, 273–297. https://doi.org/10.1081/DMR-120000653.

Giacomini, K.M., Huang, S.-M., Tweedie, D.J., Benet, L.Z., Brouwer, K.L.R., Chu, X., Dahlin, A., Evers, R., Fischer, V., Hillgren, K.M., Hoffmaster, K.A., Ishikawa, T., Keppler, D., Kim, R.B., Lee, C.A., Niemi, M., Polli, J.W., Sugiyama, Y., Swaan, P.W., Ware, J.A., Wright, S.H., Wah Yee, S., Zamek-Gliszczynski, M.J., Zhang, L., Consortium, T.I.T., 2010. Membrane transporters in drug development. Nat. Rev. Drug Discov. 9, 215–236. https://doi.org/10.1038/nrd3028.

Horie, K., Tang, F., Borchardt, R.T., 2003. Isolation and characterization of Caco-2 subclones expressing high levels of multidrug resistance protein efflux transporter. Pharm. Res. 20, 161–168. https://doi.org/10.1023/A:1022359300826.

Hu, M., Li, Y., Davitt, C.M., Huang, S.M., Thummel, K., Penman, B.W., Crespi, C.L., 1999. Transport and metabolic characterization of Caco-2 cells expressing CYP3A4 and CYP3A4 plus oxidoreductase. Pharm. Res. https://doi.org/10.1023/A:1018986605929.

Ichikawa, M., Akamine, H., Murata, M., Ito, S., Takayama, K., Mizuguchi, H., 2021. Generation of tetracycline-controllable CYP3A4-expressing Caco-2 cells by the piggyBac transposon system. Sci. Rep. 11, 11670. https://doi.org/10.1038/s41598-021-91160-z.

Imai, T., Imoto, M., Sakamoto, H., Hashimoto, M., 2005a. Identification of esterases expressed in Caco-2 Cells and effects of their hydrolyzing activity in predicting human intestinal absorption. Drug Metab. Dispos. 33, 1185–1190. https://doi.org/10.1124/dmd.105.004226.

Imai, T., Imoto, M., Sakamoto, H., Hashimoto, Mitsuru, 2005b. Identification of esterases expressed in Caco-2 cells and effects of their hydrolyzing activity in predicting human intestinal absorption. Pharmacology 33, 1185–1190. https://doi.org/10.1124/dmd.105.004226.tion.

IMAI, T., 2006. Human carboxylesterase isozymes: catalytic properties and rational Drug Design. Drug Metab. Pharmacokinet. 21, 173–185. https://doi.org/10.2133/DMPK.21.173.

Ishizaki, Y., Furihata, T., Oyama, Y., Ohura, K., Imai, T., Hosokawa, M., Akita, H., Chiba, K., 2018. Development of a Caco-2 cell line carrying the human intestine-type CES expression profile as a promising tool for Ester-containing drug permeability studies. Biol. Pharm. Bull. 41, 697–706. https://doi.org/10.1248/BPB.B17-00880.

Jin, X., Luong, T.-L., Reese, N., Gaona, H., Collazo-Velez, V., Vuong, C., Potter, B., Sousa, J.C., Olmeda, R., Li, Q., Xie, L., Zhang, J., Zhang, P., Reichard, G., Melendez, V., Marcsisin, S.R., Pybus, B.S., 2014. Comparison of MDCK-MDR1 and Caco-2 cell based permeability assays for anti-malarial drug screening and drug

investigations. J. Pharmacol. Toxicol. Methods 70, 188–194. https://doi.org/10.1016/j.vascn.2014.08.002.

Kataoka, M., Terashima, Y., Mizuno, K., Masaoka, Y., Sakuma, S., Yokoi, T., Yamashita, S., 2013. Establishment of MDCKII cell monolayer with metabolic activity by CYP3A4 transduced with recombinant adenovirus. Drug Metab. Pharmacokinet. 28, 125–131. https://doi.org/10.2133/dmpk.DMPK-12-RG-059.

Kawabata, K., Sakurai, F., Yamaguchi, T., Hayakawa, T., Mizuguchi, H., 2005. Efficient gene transfer into mouse embryonic stem cells with adenovirus vectors. Mol. Ther. 12, 547–554. https://doi.org/10.1016/j.ymthe.2005.04.015.

Kwatra, D., Budda, B., Vadlapudi, A.D., Vadlapatla, R.K., Pal, D., Mitra, A.K., 2012. Transfected MDCK cell line with enhanced expression of CYP3A4 and P-glycoprotein as a model to study their role in drug transport and metabolism. Mol. Pharm. 9, 1877–1886. https://doi.org/10.1021/mp200487h.

de Man, F.M., Goey, A.K.L., van Schaik, R.H.N., Mathijssen, R.H.J., Bins, S., 2018. Individualization of Irinotecan treatment: a review of pharmacokinetics, pharmacodynamics, and pharmacogenetics. Clin. Pharmacokinet. https://doi.org/10.1007/s40262-018-0644-7.

McLeod, D.C., Cleary, J.D., Taylor, J.W., 1986. Enalapril: a new angiotensin converting enzyme inhibitor. Drug Intell. Clin. Pharm. 20, 177–186. https://doi.org/10.1177/106002808602000301.

Mease, K., Sane, R., Podila, L., Taub, M.E., 2012. Differential selectivity of efflux transporter inhibitors in Caco-2 and MDCK–MDR1 monolayers: a strategy to assess the interaction of a new chemical entity with P-gp, BCRP, and MRP2. J. Pharm. Sci. 101, 1888–1897. https://doi.org/10.1002/jps.23069.

Nauli, M.A., Nauli, M.S., 2013. Intestinal transport as a potential determinant of drug bioavailability. Curr. Clin. Pharmacol. https://doi.org/10.2174/1574884711308030012.

Negoro, R., Yamada, N., Watanabe, K., Kono, Y., Fujita, T., 2022. Generation of Caco-2 cells stably expressing CYP3A4·POR·UGT1A1 and CYP3A4·POR·UGT1A1*6 using a PITCh system. Arch. Toxicol. 96, 499–510. https://doi.org/10.1007/s00204-021-03175-0.

Nishimuta, H., Sato, K., Yabuki, M., Komuro, S., 2011. Prediction of the intestinal first-pass metabolism of CYP3A and UGT substrates in humans from in vitro data. Drug Metab. Pharmacokinet. 26, 592–601. https://doi.org/10.2133/dmpk.DMPK-11-RG-034.

Paine, M.F., Hart, H.L., Ludington, S.S., Haining, R.L., Rettie, A.E., Zeldin, D.C., 2006. The human intestinal cytochrome P450 "pie. Drug Metab. Dispos. 34, 880–886. https://doi.org/10.1124/dmd.105.008672.

Prueksaritanont, T., Gorham, L.M., Hochman, J.H., Tran, L.O., Vyas, K.P., 1996. Comparative studies of drug-metabolizing enzymes in dog, monkey, and human small intestines, and in Caco-2 cells. Drug Metab. Dispos. 24.

Ran, F.A., Hsu, P.D., Wright, J., Agarwala, V., Scott, D.A., Zhang, F., 2013. Genome engineering using the CRISPR-Cas9 system. Nat. Protoc. 8, 2281–2308. https://doi.org/10.1038/nprot.2013.143.

Shintani, T., Imamura, C., Ueyama-Toba, Y., Inui, J., Watanabe, A., Mizuguchi, H., 2023. Establishment of UGT1A1-knockout human iPS-derived hepatic organoids for UGT1A1-specific kinetics and toxicity evaluation. Mol. Ther. Methods Clin. Dev. 30, 429–442. https://doi.org/10.1016/j.omtm.2023.08.003.

Sun, H., Chow, E.C.Y., Liu, S., Du, Y., Pang, K.S., 2008. The Caco-2 cell monolayer: usefulness and limitations. Expert Opin. Drug Metab. Toxicol. 4, 395–411. https://doi.org/10.1517/17425255.4.4.395.

Takayama, K., Igai, K., Hagihara, Y., Hashimoto, R., Hanawa, M., Sakuma, T., Tachibana, M., Sakurai, F., Yamamoto, T., Mizuguchi, H., 2017. Highly efficient biallelic genome editing of human ES/iPS cells using a CRISPR/Cas9 or TALEN system. Nucleic Acids Res. 45, 5198–5207. https://doi.org/10.1093/nar/gkx130.

Takenaka, T., Harada, N., Kuze, J., Chiba, M., Iwao, T., Matsunaga, T., 2016. Application of a human intestinal epithelial cell monolayer to the prediction of oral drug absorption in humans as a superior alternative to the Caco-2 cell monolayer. J. Pharm. Sci. 105, 915–924. https://doi.org/10.1016/j.xphs.2015.11.035.

Takenaka, T., Kazuki, K., Harada, N., Kuze, J., Chiba, M., Iwao, T., Matsunaga, T., Abe, S., Oshimura, M., Kazuki, Y., 2017. Development of Caco-2 cells co-expressing CYP3A4 and NADPH-cytochrome P450 reductase using a human artificial chromosome for the prediction of intestinal extraction ratio of CYP3A4 substrates. Drug Metab. Pharmacokinet. 32, 61–68. https://doi.org/10.1016/j.dmpk.2016.08.004.

Taketani, M., Shii, M., Ohura, K., Ninomiya, S., Imai, T., 2007. Carboxylesterase in the liver and small intestine of experimental animals and human. Life Sci. 81, 924–932. https://doi.org/10.1016/j.lfs.2007.07.026.

Temple, C.S., Boyd, C.A.R., 1998. Proton-coupled oligopeptide transport by rat renal cortical brush border membrane vesicles: a functional analysis using ACE inhibitors to determine the isoform of the transporter. Biochim. Biophys. Acta Biomembr. 1373, 277–281. https://doi.org/10.1016/S0005-2736(98)00093-5.

Thomsen, R., Rasmussen, H.B., Linnet, K., 2014. In vitro drug metabolism by human carboxylesterase 1: focus on Angiotensin-converting enzyme inhibitors. Drug Metab. Dispos. 42, 126–133. https://doi.org/10.1124/DMD.113.053512.

Wilkinson, G.R., 2005. Drug metabolism and variability among patients in drug response. N. Engl. J. Med. 352, 2211–2221. https://doi.org/10.1056/NEJMra032424.

Yamada, N., Negoro, R., Watanabe, K., Fujita, T., 2023. Generation of Caco-2 cells with predictable metabolism by CYP3A4, UGT1A1 and CES using the PITCh system. Drug Metab. Pharmacokinet. 50, 100497. https://doi.org/10.1016/j.dmpk.2023.100497.

Yamashita, S., Konishi, K., Yamazaki, Y., Taki, Y., Sakane, T., Sezaki, H., Furuyama, Y., 2002. New and better protocols for a short-term Caco-2 cell culture system. J. Pharm. Sci. 91, 669–679. https://doi.org/10.1002/jps.10050.

Yusa, K., Zhou, L., Li, M.A., Bradley, A., Craig, N.L., 2011. A hyperactive piggyBac transposase for mammalian applications. Proc. Natl. Acad. Sci. U. S. A. 108, 1531–1536. https://doi.org/10.1073/pnas.1008322108.